Received 19 October 2022; revised 15 November 2022; accepted 20 November 2022. Date of publication 28 November 2022;
date of current version 14 December 2022.

Digital Object Identifier 10.1109/OJAP.2022.3225169

An Ambient RF Powered Wireless Sensor System

MING-TAI CHIU[1], CHI-YUK CHIU[1] (Senior Member, IEEE), CHARLES NG[1], LAP-ON WONG[1], SHANPU SHEN[1] (Member, IEEE), AND ROSS MURCH[1,2] (Fellow, IEEE)

[1]Department of Electronic and Computer Engineering, The Hong Kong University of Science and Technology, Hong Kong

[2]Institute for Advanced Study, The Hong Kong University of Science and Technology, Hong Kong

CORRESPONDING AUTHOR: C.-Y. CHIU (e-mail: eefrankie@ust.hk)

This work was supported in part by the Hong Kong Research Grants Council Collaborative Research Fund under Grant C6012-20GF, and in part by the Electrical and Mechanical Services Department, the Hong Kong Special Administrative Region Government under Grant I&T Wish W-0360.

ABSTRACT The development of an ambient radio frequency (RF) powered Internet of Things (IoT) wireless sensor system is reported. The system integrates all major components including multiple antennas, rectifiers, a power management unit (PMU), a microcontroller unit (MCU) with RF transceiver module and sensing unit. A novelty of this applied engineering innovation is the design and use of multi-band dual-polarized multiple antennas to handle the low ambient RF power density found in the everyday environment. Our prototype demonstrates that it is possible to sense temperature, pressure and humidity and wirelessly transmit these signals to a central server with a duty cycle of approximately 15 minutes, when the background ambient RF signals are as low as −28.6 dBm at 950 MHz. The proposed system can address the important issue of energy supply in the development of IoT providing an alternative energy source to batteries or solar cells. Ambient RF powered IoT devices do not require periodic replacement of their batteries or to be placed in visible regions which makes them suitable for wall, ceiling and floor applications. Our ambient RF powered IoT wireless sensor system provides concrete proof, through demonstration, that harnessing ambient RF energy for powering IoT sensor systems is feasible.

INDEX TERMS Antenna array, dual-polarized, Internet of Things (IoT), multi-band, rectifier, RF energy harvesting, wireless sensor system.

I. INTRODUCTION

THE INTERNET of Things (IoT) is a key element in the next phase of the information revolution [1], [2]. IoT deployment can enable the gathering of information about the environment, our health, factories and buildings [3], [4], [5] and lead to improvements in energy efficiency and service quality [6], [7], [8].

A critical issue in the development of devices for IoT is their need for energy. Batteries are a solution that is often used, but these need to be periodically replaced, which is prohibitive when there are numerous IoT devices, or they are located in difficult to access areas. Solar cells can be used to harvest energy as a substitute for batteries but are only suitable for lighted areas and as such will also be visible in the environment. To counter this problem, various alternative energy harvesting technologies which collect energy from the environment to self-power devices have been investigated. These technologies include thermoelectric generators and piezoelectric vibration energy harvesters or some combination of them [9], [10], [11].

The wireless revolution over the past three decades has also opened up the possibility of radio frequency (RF) energy harvesting for powering IoT devices. The deployment of cellular systems and WiFi alongside existing systems such as TV and radio provide an RF signal base that can be utilized for energy harvesting virtually anywhere. We refer to this RF energy base as ambient RF in the remainder of this paper. Never before in the history of human-kind has there been such a widely accessible set of ambient RF resources [12]. Ambient RF energy harvesting is a technology that is now becoming feasible.

A major challenge of ambient RF energy harvesting is the low RF signal power available, and this is in direct contrast to wireless power transfer (WPT) [13], [14], [15], [16] where the RF source can be controlled and provide sufficient RF power. A significant limitation in the possibility of ambient

RF energy harvesting is the diode rectifier. It requires a certain turn on power, and it is inherently non-linear with its efficiency becoming very low at power levels of less than −30 dBm [17], [18], [19], [20]. Therefore, in ambient RF energy harvesting a key target of research is to maximize the RF power collected by utilizing multiple antenna elements. This requires novel multiple element antenna designs as well as novel power combining techniques.

Several power combining techniques incorporating different antenna designs have been proposed [21], [22], [23], [24]. They can be classified as DC, RF and hybrid combining. In RF combining, multiple antenna elements at the RF level are combined, in the style of an antenna array, and then rectified. The feature of this approach is that the resultant ambient RF signal is enhanced by the gain of the array and therefore the rectifier can operate at low ambient RF power levels. However, a limitation is that the array will have a narrow beamwidth and can therefore only harvest RF energy from a single direction [25]. In DC combining the signal from each individual antenna element is first rectified and then DC combined. The feature of this approach is that the patterns of the individual elements are retained and therefore it can harvest ambient RF energy over wide beamwidths [25]. The limitation is that the ambient RF power still needs to be high in order for the individual rectifiers to operate efficiently. To overcome the limitations of both approaches, hybrid combining has been proposed [24]. In this approach multiple antenna arrays are formed, each forming a main beam in a different direction. The RF output from each array is then rectified and DC combined. The resultant system can operate at low ambient RF powers while retaining energy harvesting over wide beamwidths. The drawback is that a large number of antenna elements are required. In essence, hybrid or RF combining is necessary in ambient RF energy harvesting systems in order to achieve sufficient power for the diode rectifiers to operate efficiently [24].

In previous multiple antenna designs for ambient RF energy harvesting [21], we have developed two dual-port L-probe patch antennas stacked in a back-to-back position in order to receive radiation incident from both front and back sides. In [22], we have developed a total of 16 inverted-F antennas that included four 900 MHz plus twelve 1800 MHz antenna elements. These two papers demonstrated the use of DC combining so that energy harvesting over wide beamwidths was achieved but was limited by requiring sufficient ambient RF power for the rectifiers to operate efficiently. To overcome this issue, designs with hybrid combining have also been developed. In [23], eight 2-element patch arrays were formed followed by DC combining, while in [24], four-port high gain antennas were generated from a pixel surface followed by DC combining. Cellular base station antennas are typically dual-polarized and therefore antenna designs that incorporate dual polarization for increased energy harvesting capability have also been developed [26], [27], [28] using hybrid combining.

In the design of energy harvesting systems, it is also necessary to consider the "cold" and "warm" start times. Cold start time refers to the time it takes for the energy harvesting system to become operational from when the system has zero initial energy or in other words when it is "cold". Cold starts are difficult to achieve as the initial system voltage is zero and the system must collect enough initial energy from the ambient RF power for it to become operational. Therefore, cold start times can be large and are sometimes not reported or investigated. Warm start time refers to the duty cycle time of the system once the cold start has been performed. In warm start, the system energy moves between two energy states (warm and operational energy states). In the operational energy state, the system has enough energy to power the application unit to make sensor measurements and transmit the data to a central server. At the end of the sensor measurement and transmission the system energy is depleted to the warm energy state where energy harvesting is then required to return it to the operational energy state for the next measurement. A warm start is much easier to achieve than a cold start because the power management system remains operational in the warm energy state. The warm start time is usually a fraction of the cold start time.

In this paper we report the applied engineering innovation of an ambient RF powered IoT wireless sensor system. It integrates all major components including multiple antennas, hybrid combining, rectifiers, a power management unit (PMU), a microcontroller unit (MCU) with RF transceiver module and a sensing unit. A novel feature of the design is the use of multiple antennas that are multi-banded and dual-polarized to cope with the low ambient RF power density found in everyday environments. Another novel feature is the use of off-the-shelf electronic modules so that the design can be easily prototyped and replicated by others. Hybrid combining of the antennas is utilized to obtain the necessary power for the diode rectifiers to operate efficiently. It is demonstrated that the proposed system, when powered by average background ambient RF signals of as low as −28.6 dBm at 950 MHz, is able to sense temperature, pressure and humidity and wirelessly transmit these signals to a central station with a duty cycle (or warm start time) of approximately 15 minutes and a cold start time of approximately 6 hours. A demonstration of an ambient RF power IoT system operating at this ambient RF power level using off-the-shelf components has not previously been reported to the best of the authors knowledge. Specific applied contributions of this paper include:

1) An efficient multiport antenna design consisting of 16 radiating elements divided into three frequency bands and two polarization's.
2) Designs for efficient rectifiers that are optimized for single-band 900 MHz or dual-band 1800 MHz and 2100 MHz operation.
3) The use of hybrid combining for antennas operating with different polarization's and frequency bands.

4) Integration of the multiple antennas and rectifiers with off-the-shelf electronic modules consisting of a PMU with supercapacitor, MCU with integrated Bluetooth and barometric pressure, ambient temperature and relative humidity sensors.
5) Demonstration of cold start operation for the system for ambient RF power levels of −28.6 dBm at 950 MHz with a cold start time of 6 hours.
6) Demonstration of continuous operation and communication with duty cycles (warm start time) of approximately 15 minutes for −28.6 dBm at 950 MHz ambient power operation.

The paper is organized as follows. A survey of indoor ambient RF energy levels available at The Hong Kong University of Science and Technology (HKUST) campus and a system overview of wireless sensor systems powered by ambient RF energy harvesting are provided in Section II. In Section III-A, a design for 16 antenna elements operating in three frequency bands and two polarization's is described. The design for two rectifiers operating in the single-band 900 MHz and dual-band 1800 MHz and 2100 MHz frequencies is presented in Section III-B along with the hybrid combining arrangement. The PMU and supercapacitor design for increasing voltage levels and storing energy is described in Section III-C. The description of the application unit (AU) including the collection and transmission of environmental data to a central server is given in Section III-D. In Section IV, a complete solution for a batteryless wireless sensor system which is powered by ambient RF signals is given. The corresponding field testing results carried out on a university campus are also provided. Finally, a conclusion is provided in Section V.

II. AMBIENT RF ENERGY HARVESTING SYSTEM BACKGROUND

A. AMBIENT POWER MEASUREMENTS

A variety of mobile cellular communication services across various frequency bands are available for the general public around the world. For example, the second to fifth generation (2G to 5G) cellular networks are currently provided to consumers using spectrum in the 900, 1800 and 2100 MHz bands. The exact frequency bands for downlink cellular communication in Hong Kong, as assigned by the Office of the Communications Authority (OFCA), are given in Table 1. According to the technical specification stipulated by the Third Generation Partnership Project (3GPP), the rated carrier output power ($P_{rate,c}$) of medium range and local area base stations should be $\leq +38$ dBm and $\leq +24$ dBm, respectively, where $P_{rate,c}$ of the base station is the mean power level for a specific carrier that the manufacturer has declared to be available at the antenna connector during the transmitter ON period [29].

The RF emissions from cellular systems are now present in nearly all parts of the world and form a signal base for harnessing RF energy virtually anywhere. To harness ambient RF energy, it is necessary to characterize its strength in both spatial and temporal dimensions. This has been performed by others [31] and we have also performed similar surveys around the campus of HKUST to verify the power spectrum in the associated frequency bands.

TABLE 1. Downlink frequency bands and standards for mobile services in Hong Kong [30].

Mobile Phone Receive (MHz)	Technical Standards Adopted by Mobile Operators
930 -960	GSM, UMTS, FDD-LTE
1805 - 1880	GSM, FDD-LTE
2110.3 - 2169.7	UMTS, FDD-LTE, NR FDD

Note: GSM denotes Global System for Mobile Communications (2G); UMTS denotes Universal Mobile Telecommunications Services (3G); FDD-LTE denotes Frequency Division Duplex - Long Term Evolution (4G); NR FDD denotes New Radio Frequency Division Duplex (5G).

The measurements at HKUST were carried out during normal weekday afternoons with students and staff moving around the campus. We used a Rohde & Schwarz FSH8 handheld spectrum analyzer and a wideband Double-Ridged Waveguide Horn (Model: 3115) to obtain ambient RF signal strengths over the three frequency bands listed in Table 1. In the measurement process we orient the horn antenna to the direction that provides maximum signal strength, and this usually coincides with the direction to the nearest base station. Ten indoor locations are reported in the main academic building on campus as depicted in Fig. 1. In the measurements, the data collection period at each location was 3 mins with a sampling rate of 10 samples per second, from 800 MHz to 2200 MHz. The frequency sampling interval was 2 MHz in which the root-mean-square (RMS) power levels were recorded in a Secure Digital (SD) memory card. According to the specifications provided by the manufacturer, the 3-meter calibration horn antenna gains at 1000 MHz, 1500 MHz, 2000 MHz and 2500 MHz are 4.3 dBi, 6.8 dBi, 7.0 dBi and 7.6 dBi, respectively. The cable losses at 950 MHz, 1850 MHz and 2150 MHz were found as 0.85 dB, 1.26 dB and 1.36 dB, respectively. Therefore, the average background RF signal power strengths, with respect to an omni-directional receiving antenna with unity gain (averaged RMS value - horn antenna gain + cable loss), in the three frequencies bands can be obtained and are as shown in Table 2.

In our HKUST survey shown in Table 2, we found that the received RF signal power at indoor user locations was −23 dBm on average depending on how far away the base station antennas were and whether line-of-sight propagation was present. However, the RF signal strengths in many indoor testing locations are found to be −40 dBm or less. In addition to the 3-min measurements, a 72-hour datalog taken at location L5 (computer barn) was performed as well. It was found that the available RF signal strength was also correlated to human activities at the location. From mid-night to early morning, the recorded signal had dropped by 13 dB in general when compared to the remaining 24 hour period.

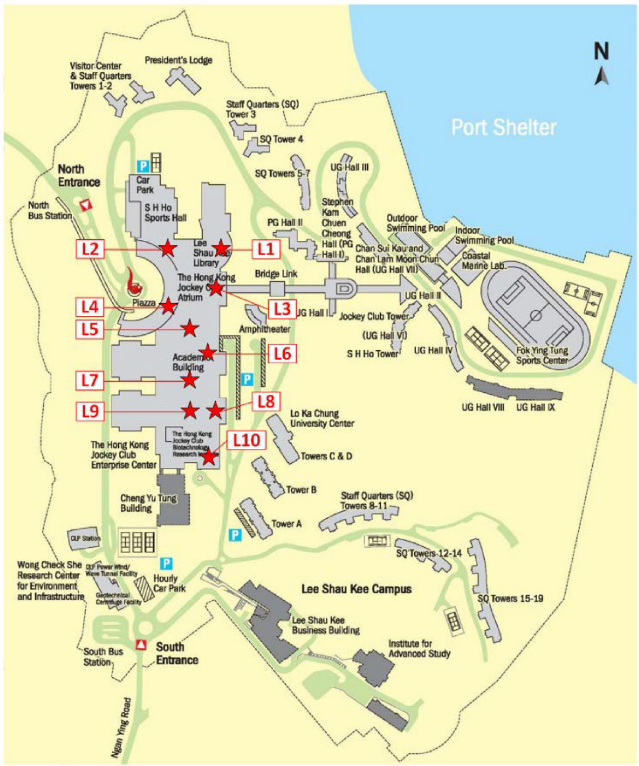

FIGURE 1. HKUST campus measurement locations L1-L10. All measurements are taken indoor the main campus building.

TABLE 2. Average background RF signal power strengths within a frequency band measured at HKUST campus.

Location no. (Details)	Band 1 (dBm)	Band 2 (dBm)	Band 3 (dBm)
#L1 (G/F, Library)	−44.48	−44.25	−52.90
#L2 (G/F, Atrium)	−32.96	−41.07	−44.45
#L3 (LG1, Cafe Entrance)	−35.31	−40.63	−37.69
#L4 (3/F, Upper Atrium)	−43.99	−54.85	−60.67
#L5 (4/F, Computer Barn)	−26.19	−41.03	−44.88
#L6 (6.5/F, Staircase)	−23.28	−27.37	−35.52
#L7 (7/F, Corridor)	−28.34	−30.48	−49.09
#L8 (3/F, Research Office)	−35.31	−40.63	−37.69
#L9 (1/F, Concourse)	−46.29	−60.58	−58.48
#L10 (6/F, Lecture Room)	−37.24	−33.60	−46.72

Note: Band 1 denotes band 930 - 960 MHz; Band 2 denotes band 1805 - 1880 MHz; Band 3 denotes band 2110 - 2170 MHz; G/F denotes ground floor; LG1 denotes lower ground 1/F.

More details are provided in the performance section of this paper.

It is interesting to benchmark our findings with previous surveys and here we compare it to an ambient RF spectral survey undertaken outside 270 London Underground stations at street level (outdoor environment) [31]. According to the average band RF power density provided in [31], the average

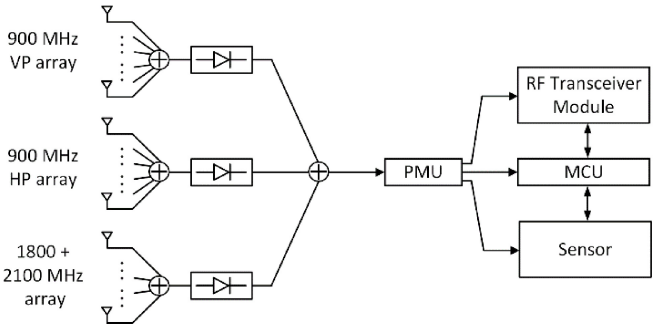

FIGURE 2. Block diagram of the proposed ambient RF powered wireless sensor system. From left to right the components are respectively the antennas, rectifiers, PMU and AU (MCU, Sensors and RF transceiver module).

available signal strengths (again with respect to an omnidirectional receiving antenna with unity gain) at the bands of 925 - 960 MHz, 1805 - 1880 MHz and 2110 - 2170 MHz were −25.37 dBm, −27.51 dBm and −37.27 dBm, respectively. The corresponding signal power levels are comparable to those obtained at the best location (#L6) with respect to the same frequency band in our survey of the indoor campus environment.

B. SYSTEM OVERVIEW

The wireless sensor system powered by ambient RF energy harvesting can be divided into four sub-systems consisting of the antenna, rectifier, PMU and AU as shown in Fig. 2. The purpose of the antenna is to collect as much ambient RF power as possible for the size of the device over as many polarization's and frequencies as possible. The rectifiers should be as efficient as possible and operate efficiently at as low power as possible (−30 dBm). The term rectenna is also commonly used to describe a receiving antenna that is used for converting RF into DC. Recently, multiple bands, linearly polarized, circularly polarized and several key design requirements for developing rectennas used for ambient RF energy harvesting have been proposed and described in the literature [32], [33], [34], [35]. The PMU collects the DC power from the rectifiers and utilizes an energy storage element consisting of a supercapacitor. When the energy stored is large enough, the PMU would allow the energy to be released to the AU. The AU consists of an MCU, communication and sensors matched to the particular application of interest. Low power MCU often have communication embedded including Bluetooth low energy (BLE), so there is often no need for an external RF transceiver module. Sensors are connected to the MCU and the sampled signals are then processed. After powering up, the AU would turn on the sensors attached, collect data from them and transmit it to a server. Due to the low signal power available in the ambient RF spectrum, the system targets low-duty cycle type applications such as the slowly varying parameters of temperature, pressure and humidity in the environment.

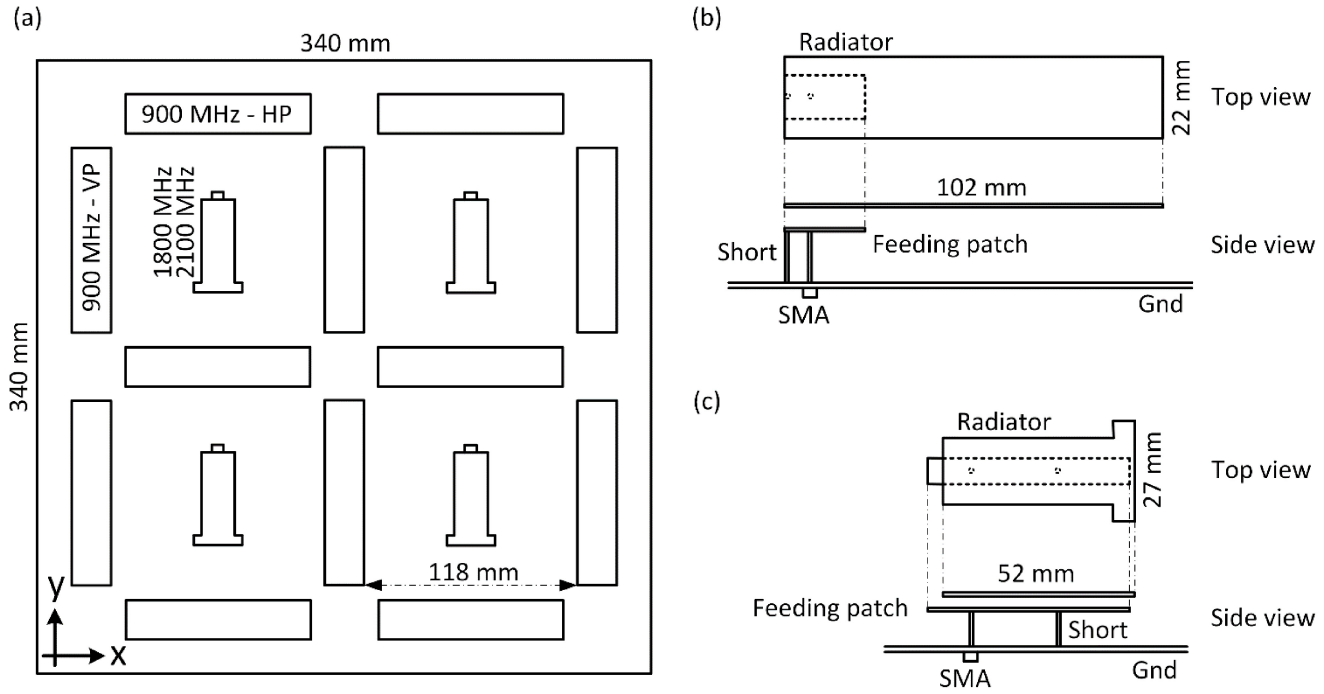

FIGURE 3. Geometry of the proposed multi-band dual-polarized patch antenna array: (a) top view; (b) 900 MHz antenna element; and (c) 1800 & 2100 MHz antenna element.

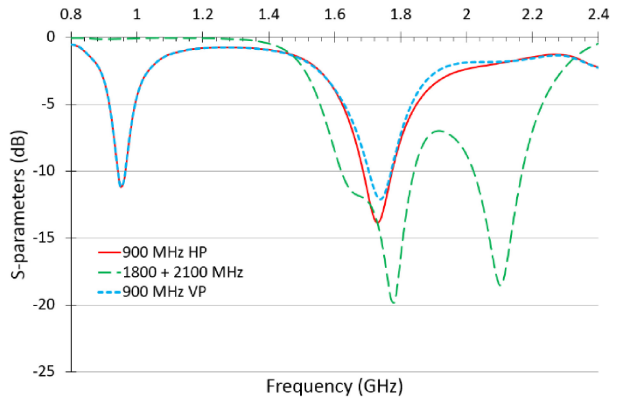

FIGURE 4. Simulated reflection coefficients of the proposed multi-band dual-polarized patch antenna array with ideal power combining.

III. SYSTEM COMPONENTS

Details of the design for each of the components shown in Fig. 2 are described in the following sections.

A. MULTI-BAND DUAL-POLARIZED PATCH ANTENNA ARRAY

Figure 3 shows the overall layout and the individual elements of the proposed multi-band dual-polarized patch antenna array. The array consists of 16 antenna elements in total situated on a 340 mm x 340 mm ground plane as shown in Fig. 3(a). There are two sets of six rectangular patch antennas operating in the 900 MHz band where they are oriented in horizontal and vertical positions. The remaining four smaller patch antennas are for dual-band 1800 MHz and 2100 MHz operation and are inserted between the 900 MHz patch antennas. In this way three separate antenna arrays are created according to their patch size and orientation. We refer to these as the 900 MHz horizontally polarized (HP) array, 900 MHz vertically polarized (VP) array and dual-band 1800 MHz and 2100 MHz array. Figure 3(b) shows the enlarged structure of the 900 MHz patch antenna element. The antenna consists of one radiator suspended in air 20 mm above the ground plane. It is capacitively excited [36] by a shorted feeding patch (22 mm x 14 mm) 5.5 mm underneath. The dual-band antenna element is also shown in Fig. 3(c). The top T-shaped radiator is suspended in air 13.5 mm above the ground plane. Similarly, it is also capacitively excited by a shorted feeding patch (54.5 mm x 7 mm) 3.1 mm underneath. It should be noted that all antenna elements are built from 1 mm-thick copper plates and copper rods without incorporating any substrate boards.

In order to generate high gain radiation beams in the broadside direction, three separate feeding networks are required for combining the three sets of arrays (900 MHz HP array, 900 MHz VP array and dual-band 1800 MHz and 2100 MHz array). Since our focus is utilizing off-the-shelf components, we have selected three RF power combiners for our prototype. The combiners we use are two 6-to-1 (model: ZB6PD-17-S, 6 Way-0°, 50W, 600 to 1700 MHz) and one 4-to-1 (ZN4PD- 272-S+, 4 Way-0°, 50W, 500 to 2700 MHz) from Mini-Circuits [37]. The simulated reflection coefficients of the three antenna arrays are given in Fig. 4, in which the post-processing step of "Combine Results" in the CST simulation [38] is used to simulate ideal combining.

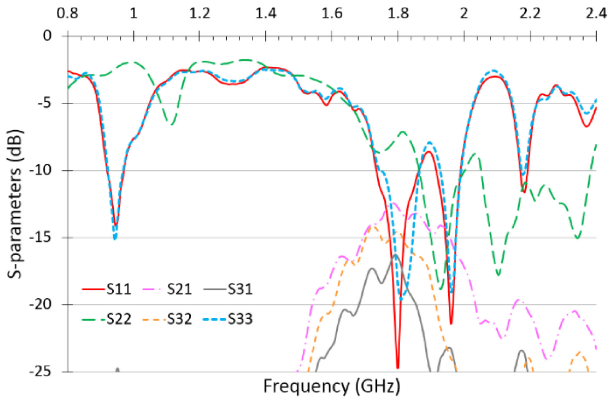

FIGURE 5. Measured *S*-parameters of the proposed multi-band dual-polarized patch antenna array using power combiners. Ports 1, 2 and 3 refer to the antenna ports of 900 MHz HP array, dual-band 1800 MHz and 2100 MHz array, and 900 MHz VP array, respectively.

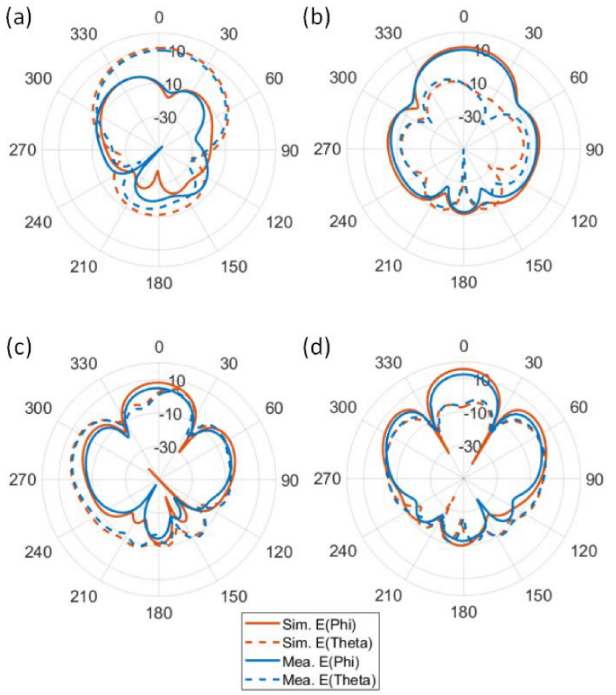

FIGURE 6. Simulated and measured radiation patterns of the proposed multi-band dual-polarized patch antenna array: (a) HP array at 950 MHz; (b) VP array at 950 MHz; (c) dual-band array at 1850 MHz; and (d) dual-band array at 2150 MHz.

The corresponding measurement results incorporating the off-the-shelf RF power combiners are provided in Fig. 5. Ports 1, 2 and 3 refer to the antenna ports of 900 MHz HP array, dual-band 1800 MHz and 2100 MHz array, and 900 MHz VP array, respectively. The simulated and measurement results agree closely with each other though certain ripples are exhibited in the experiment due to the use of physical combiners and cables, closely spaced antenna elements and imperfect fabrication of individual radiating elements. It should be noted that the two 900 MHz arrays also exhibit 1800 MHz resonances, but their radiation performance is not guaranteed owing to the specified frequency range of

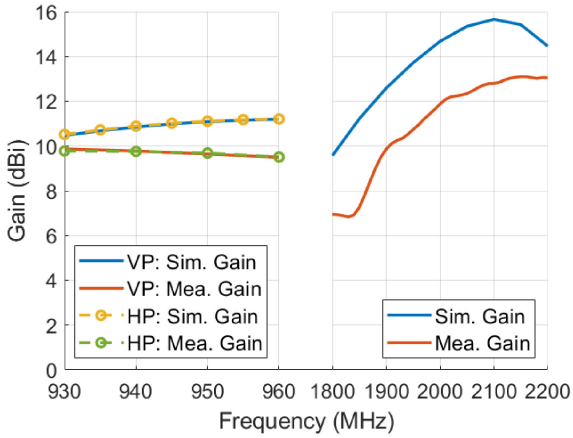

FIGURE 7. Simulated and measured antenna array gains. The discrepancy is due to the use of physical combiners and cables, closely spaced antenna elements and imperfect fabrication of individual radiating elements in measurement.

RF power combiners used. In addition, it should be noted that due to the doubling of the electrical length of the element spacing at 1800 MHz, a relatively narrower array beam pattern will be produced. Nevertheless, it is still possible to use the proposed two 900 MHz HP and VP arrays to capture 1800 MHz signals as well if the associated power combiners and rectifiers can be modified accordingly.

The simulated and measured radiation patterns of the proposed antenna array cut in the *xz*-plane are provided in Fig. 6. These patterns include HP array at 950 MHz, VP array at 950 MHz, and dual-band array at 1850 MHz and 2150 MHz. All antenna arrays show broadside radiation with measured gains and efficiencies of 9.7 dBi, 62%, 9.7 dBi, 66%, 7.3 dBi, 37%, 13.1 dBi, 61%, respectively. The simulated and measured antenna array gains are also given in Fig. 7.

B. SINGLE- AND DUAL-BAND RECTIFIERS

An efficient rectifier is crucial to convert the collected RF signals into DC signals for the energy harvesting system to be useful. To design a rectifier, a number of considerations need to be taken into account. Firstly, an appropriate diode should be selected. Since the proposed system collects RF energy from the environment in which the target input RF power would be -20 to -30 dBm range (input power of the antenna array), a low turn-on voltage is essential. Secondly, to match with the antenna characteristics, a single band or multi-band operation rectifier should be developed accordingly. Thirdly, as the optimum load of the rectifier varies with both frequency and input power, the load resistor should be optimized under the specified user condition during the design process. Finally, various rectifier configurations are available, such as single series, voltage doubler, and diode bridge topologies with a tradeoff for circuit complexity and performance [39].

Two kinds of rectifiers need to be developed with one operating at the single 900 MHz band and another in the

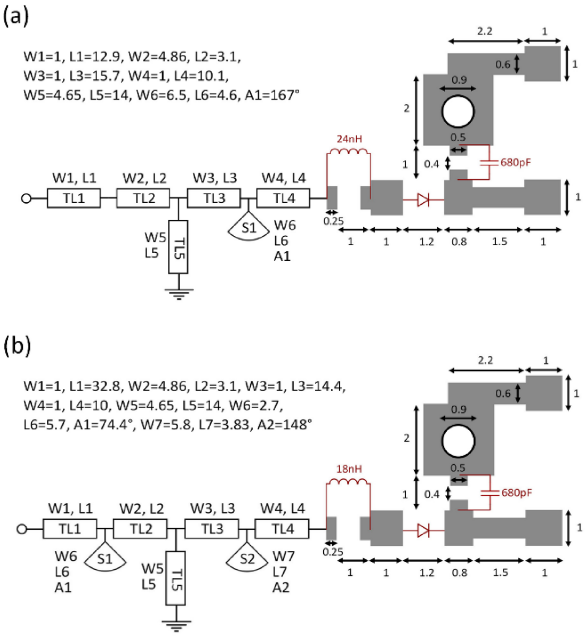

FIGURE 8. Topology layouts of rectifiers for (a) single band 900 MHz range; (b) dual-band 1800 & 2100 MHz ranges (units: mm).

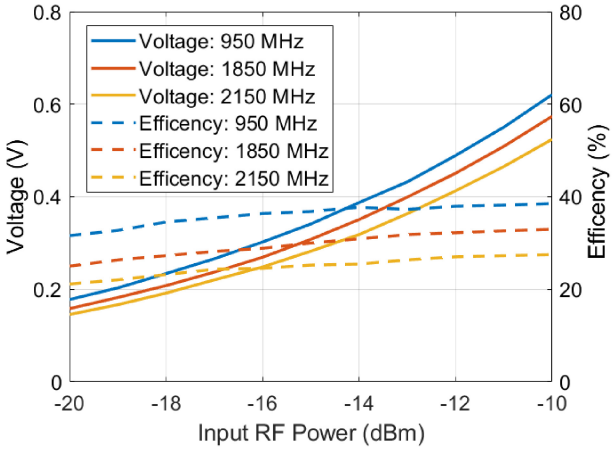

FIGURE 9. Measured output voltage and RF-to-DC efficiency of the proposed single band and dual-band rectifiers.

dual-band 1800 MHz and 2100 MHz ranges. Figure 8 shows the schematic diagram of our proposed rectifiers which include distributed microstrip stubs, radial filters, and discrete components of capacitors, inductors and diodes. The radial stubs were used in our rectifier circuit design because 1) the radial stubs act as low pass filters for suppressing the sinusoidal terms of the output voltage and output current; 2) compared to a quarter-wavelength straight stub, a radial stub will have a smaller insertion point which is more precise for determining the insertion location during calculation; and 3) a radial stub has a low-impedance point over a wider frequency range compared to the quarter-wavelength straight stub which implies a wideband characteristic [40]. The design structures are referenced to [21] and the corresponding key dimensions and discrete component values are listed in the figure. The single series diode topology was selected because of its straightforward design and high RF-to-DC conversion efficiency at low input powers. The non-linear device we used in the rectifier construction was Schottky diode HSMS-2850 from Avago Technologies. The substrate used was RT/Duroid 5880 with relative permittivity of 2.2 and thickness 62 mil.

The ultimate goal of our system is to harvest ambient RF energy to power up a wireless sensor system for monitoring slow varying parameters. If the RF power level in the environment is too low, it would not be adequate to let the entire system function. With the inclusion of 10 dBi antenna array gain, it is reasonable to assume that the operating RF input power range of the rectifier would be −10 to −20 dBm (see location L5 in Table 2 for example). Figure 9 shows the measured conversion efficiency of the two proposed rectifiers at the designated frequencies. The RF-to-DC efficiencies exhibit an increment of a few percent over the target input power range due to the non-linear characteristics of the diodes. In our system design, two sets of 900 MHz antenna arrays and one set of dual-band 1800 MHz and 2100 MHz antenna array are used. Therefore, a total of three rectifiers are needed and their DC outputs are combined together in parallel and input to the PMU. Due to the uncontrollable signals from the environment, a parallel connection can provide a more stable power supply in case there is any significant drop with one rectifier's output.

C. POWER MANAGEMENT UNIT

The next stage is to devise the remaining components of the wireless sensor system that can store and use the energy converted from the ambient RF signals. A PMU is employed to handle the energy storage and release energy for sensing and data uploading. This is because the harvested power from ambient RF signals is varying and unregulated which is not ideal for charging or for direct use. In addition, the PMU consists of a key component which is the voltage booster to deal with the cold start situation. When the input voltage generated from the ambient RF harvesting is low and unsteady, the threshold voltage of turning on the power management integrated circuit is difficult to achieve. Therefore, a voltage booster is required to step-up the input voltage to a given level. In our system prototyping, the ultra low power management integrated circuit BQ25570 from Texas Instruments [41] has been selected as the PMU. It includes a nano power boost charger and this is accomplished by charging and discharging an external inductor (22 mH). As a result, the voltage booster allows the input voltage to be maintained at a level which can let the PMU start up and continue to operate. In addition, the maximum power point tracking (MPPT) technique has been adopted in the selected PMU which can optimize the extraction of energy harvested from the environment by varying its load to match with the source continuously. We utilize BQ25570 straightforwardly in our system by directly using the associated evaluation board (TI BQ25570EVM-206 Ultra Low Power Management

IC, Boost Charger Nanopowered Buck Converter Evaluation Module [42]).

For the PMU energy storage supercapacitor, the usable energy for sensor applications and data uploading can be obtained using

$$E_{usable} = \frac{1}{2}C\left(V_A^2 - V_T^2\right) \tag{1}$$

where C is the capacitance of the supercapacitor. V_A and V_T are the voltages across the supercapacitor for triggering the sensor as well as RF transceiver and the resultant voltage after data transmission is completed, respectively. From (1), the criteria for selecting the supercapacitor is that the value should be large enough to meet the demand of the AU, but it should not be too large as the cold start time would be too big. This is because when the supercapacitor voltage is low, the MPPT technique cannot optimize its load effectively resulting in low PMU efficiency. Thus if a large supercapacitor is used, it may not be possible, or it may take a very long time, to perform a cold start. The optimized value of the supercapacitor in this system is 47 mF, where the corresponding V_A and V_T are 2.73 V and 2.42 V, respectively. The resultant energy for cold start and warm start can be calculated as 175 mJ and 38 mJ. For an ideal energy harvesting system with 100% efficiency, the corresponding charge time at −20 dBm input would be 292 minutes for a cold start and 63 minutes for a warm start.

D. APPLICATION UNIT

The AU utilizes a low energy MCU with an embedded RF transceiver module. We have selected the integrated circuit CC2640R2F-Q1, which supports BLE5, from Texas Instruments. We utilize the integrated circuit straightforwardly in our system by directly using the associated development board (TI LAUNCHXL-CC2640R2 SimpleLink Bluetooth Low Energy CC2640R2 wireless MCU LaunchPad development kit [43]). Although the data rate of BLE is relatively low compared to most current wireless technologies, this would not be a critical concern as this system targets low-duty cycle wireless sensors for monitoring slowly varying parameters. In addition, BLE has low power consumption and is widely installed in mobile devices and allows the public to obtain the sensor data in a convenient way.

The low power consumption environmental sensor we use is the integrated circuit BME280 from Bosch Sensortec [44] which is able to measure barometric pressure, ambient temperature and relative humidity simultaneously. We utilize the integrated circuit straightforwardly in our system by directly using the associated development board (Adafruit BME280 I2C [45]). Once data is collected by the sensor, it can be uploaded to a central station for further processing. In a wireless sensor network (WSN), a central station can be used to gather multiple information from multiple sensor nodes via different wireless protocols. In this work, a Raspberry Pi 4 Model B [46] acts as a central station located 20 meters away from the proposed system to receive and display the environmental data.

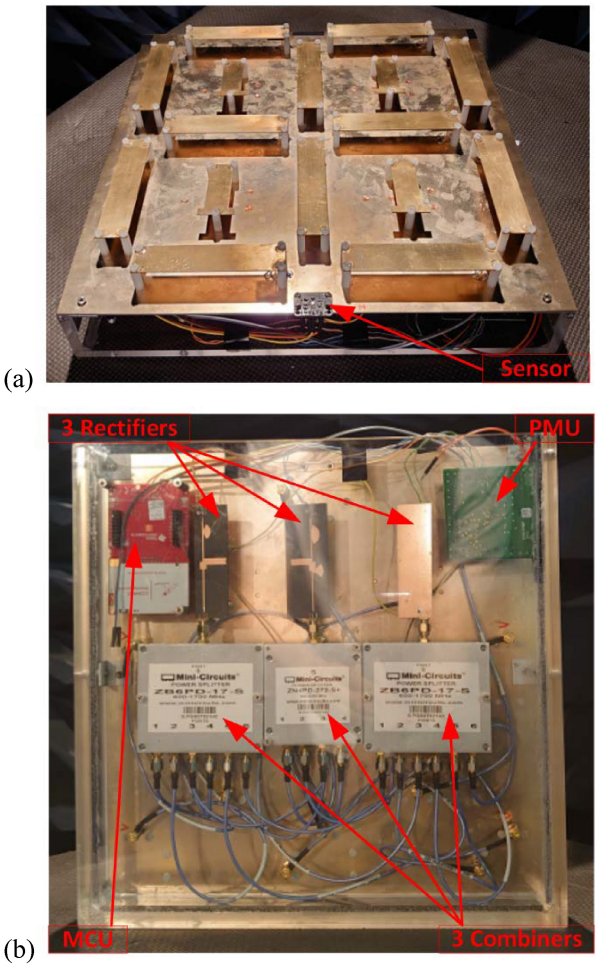

FIGURE 10. Prototype of proposed multi-band dual-polarized ambient RF powered wireless sensor system: (a) 3D view; (b) backside view where key modules are also identified (Prototype volume including antennas and acrylic box: 34 x 34 x 7.2 cm^3).

IV. AMBIENT RF POWERED WIRELESS SENSOR SYSTEM PERFORMANCE

Figure 10 shows the final prototype of the proposed multi-band dual-polarized ambient RF powered wireless sensor system. The multiple antenna arrays and the sensor module are located on the top as depicted in Fig. 10(a), while RF power combiners, rectifiers, PMU and MCU with RF transceiver module are placed under the antenna ground plane as illustrated in Fig. 10(b).

To characterize the performance of our multi-band dual-polarized ambient RF powered wireless sensor system we provide detailed measurements from location L5 (computer barn) shown in Fig. 1 and Fig. 11. This includes measurements of the raw RF power received as well as the cold start time and duty cycle (warm start time) of the system.

The ambient RF signal strength received by the proposed multiband dual-polarized patch antenna array has been

TABLE 3. Comparison of wireless sensor systems powered by RF energy harvesting.

	[47]	[48]	[49]	[50]	This work
Antenna size (cm^2)	30 x 28.65	38 x 3.8	7 x 6.6	20 x 17.5	34 x 34
Operating Freq. Band (MHz)	550	466	900/ 2025/ 2360	915	900/ 1800/ 2100
Antenna size (λ)*	0.55 x 0.53	0.59 x 0.06	0.21 x 0.20 (900 MHz)	0.61 x 0.53	1.08 x 1.08 (950 MHz)
Mea. Antenna Gain (dBi)	7.3	3.2	1.0 (900 MHz) 2.6 (2025 MHz) −0.19 (2360 MHz)	7.5	9.7 (950 MHz) 7.3 (1850 MHz) 13.1 (2150 MHz)
Average Ambient Power Level (dBm)	−13.92	−12 to 6.9	−10 (900 MHz) −10 (2025 MHz) −10 (2360 MHz)	−22 to 4	−28.58 (950 MHz) −48.49 (1850 MHz) −51.45 (2150 MHz)
Mea. Rectifier Conversion Eff. (%)†	13	5.5 to 15	N/A (900 MHz) 48 (2025 MHz) N/A (2360 MHz)	N/A	39 (950 MHz) 33 (1850 MHz) 28 (2150 MHz)
Sensor Type	N/A	Organic electrochromic device	Temperature	N/A	Pressure, temperature, and humidity
Distance Away from RF Source (m)	5600 (Base station)	0.13 (Walkie talkie)	N/A (Signal generator)	1.52 (Signal generator)	50 (Base station)
Testing Venue	Outdoor (Rooftop)	Lab	Lab	Lab	Indoor (Computer barn)
Data Uploaded Wirelessly	No	No	Yes	No	Yes
Time for Cold Start (hrs)	N/A	N/A	N/A	N/A	6
Time for Warm Start (mins)	0.17	N/A	N/A	N/A	15

*λ is the wavelength in air.
† Input RF power at -10 dBm.

FIGURE 11. Field test measurement of the multi-band dual-polarized ambient RF powered wireless sensor inside the computer barn in the HKUST campus at location L5 (see Figure 1). The base station (outside window at top left) is approximately 50 m away and our system is seen in the bottom right silhouetted in the foreground of the window. The system was entirely powered by the ambient RF cellular signals in the environment.

logged for 72 hours using a Rohde & Schwarz FSH8 handheld spectrum analyzer at the three frequency bands of interest. The antenna array was placed next to a window where it was 50 meters away from the cellular base station antennas. The signal statistics are presented in Fig. 12 and show that the 950 MHz signal was dominant in the environment. About two fifths of the time, the signal strength fell into the range of −15 to −19 dBm (including the proposed antenna array gain). There was a similar occurrence between −20 to −24 dBm. The 1850 MHz signal was nearly always between −35 to −39 dBm, while the 2150 MHz signal strength was mainly below −40 dBm.

To obtain measurements of the cold start and duty cycle (warm start) performance of the sensor system, our system prototype was used to monitor three environmental parameters including barometric pressure, ambient temperature and relative humidity. Under this configuration, the results show that the proposed system can perform a cold start in 6 hours and a warm start in 15 minutes. This means that the central station (Raspberry Pi) received the first set of data after 6 hours from when the supercapacitor was fully discharged. The sensor data was then transmitted approximately four times an hour. In fact, the time required for both cold start and warm start can be further reduced at some locations if the signal strengths of the other two frequency

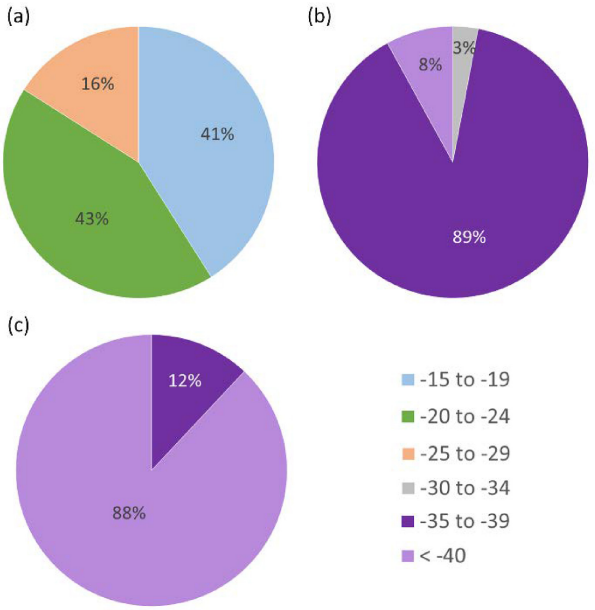

FIGURE 12. 72-hour datalog of ambient RF power strengths measured in computer barn at HKUST campus: (a) 950 MHz; (b) 1850 MHz; and (c) 2150 MHz (units: dBm).

bands (1800 MHz and 2100 MHz) in the environment are higher.

A comparison of wireless sensor systems powered by RF energy harvesting is also given in Table 3. It should be noted that the systems of [48], [49], [50] were not tested under real situations. Instead, they used dedicated sources; either walkie talkie or a signal generator, to provide RF signals for the measurement in the laboratory. Unlike the testing setup of [47] where it was performed at the rooftop to collect ambient digital TV signals, our system was located indoor to harvest energy from ambient cellular base station signals which have 14.7 dB less power available even at the dominant frequency (950 MHz). One key tradeoff in our system is the larger size compared to other systems as shown in Table 3. Due to the low ambient power in our application (compared to the other systems in Table 3) it is a necessary tradeoff in order to acquire the required RF power for efficient rectifier operation. As part of our system demonstration we can conclude that the multi-band dual-polarized patch antenna array utilized in our system is essential and has performed a tradeoff in size to cope with the low ambient RF power. Application of ambient RF energy harvesting in IoT applications therefore needs to take this size constraint into account.

V. CONCLUSION

A complete design for an ambient RF powered wireless sensor system has been described in this paper and the results from a prototype of the system have also been reported. To maximize the collected power from the ambient RF environment, multiple features have been incorporated in the antenna design. These include high gain, triple band and dual polarization with hybrid combining. Results from a particular location (an indoor environment on campus next to a window) with average background ambient RF signals as low as −28.6 dBm at 950 MHz have been reported in detail. In this location, barometric pressure, ambient temperature and relative humidity of the environment have been successfully obtained and wirelessly transmitted to a central station every 15 minutes. Even for the cold start configuration, where the energy storage (supercapacitor) is fully discharged, the first transmission of sensor data can be received at the central station in 6 hours. The time required for sensor data updates will be shorter if the available signal strengths in the frequency bands of 1800 MHz and 2100 MHz are comparable to that of the 900 MHz band. This paper provides a reference and practical demonstration of an energy harvesting system that utilizes ambient RF signals to power up IoT sensors. It provides concrete evidence that ambient RF energy harvesting can be considered as a useful energy source for IoT systems which mitigates the need for battery replacement.

REFERENCES

[1] G. Kortuem and F. Kawsar, "Market-based user innovation in the Internet of Things," in *Proc. IEEE Internet Things (IOT)*, Tokyo, Japan, Nov. 2010, pp. 1–8.
[2] M. Zorzi, A. Gluhak, S. Lange, and A. Bassi, "From today's INTRAnet of things to a future Internet of Things: A wireless-and mobility-related view," *IEEE Wireless Commun.*, vol. 17, no. 6, pp. 44–51, Dec. 2010.
[3] S. D. T. Kelly, N. K. Suryadevara, and S. C. Mukhopadhyay, "Towards the implementation of IoT for environmental condition monitoring in homes," *IEEE Sensors J.*, vol. 13, no. 10, pp. 3846–3853, Oct. 2013.
[4] C. S. Abella et al., "Autonomous energy-efficient wireless sensor network platform for home/office automation," *IEEE Sensors J.*, vol. 19, no. 9, pp. 3501–3512, May 2019.
[5] M. A. Jamshed, K. Ali, Q. H. Abbasi, M. A. Imran, and M. Ur-Rehman, "Challenges, applications and future of wireless sensors in Internet of Things: A review," *IEEE Sensors J.*, vol. 22, no. 6, pp. 5482–5494, Mar. 2022.
[6] A. Fuller, Z. Fan, C. Day, and C. Barlow, "Digital twin: Enabling technologies, challenges and open research," *IEEE Access*, vol. 8, pp. 108952–108971, 2020.
[7] A. El Saddik, F. Laamarti, and M. Alja'Afreh, "The potential of digital twins," *IEEE Instrum. Meas. Mag.*, vol. 24, no. 3, pp. 36–41, May 2021.
[8] G. Mylonas, A. Kalogeras, G. Kalogeras, C. Anagnostopoulos, C. Alexakos, and L. Muñoz, "Digital twins from smart manufacturing to smart cities: A survey," *IEEE Access*, vol. 9, pp. 143222–143249, 2021.
[9] J. Colomer, J. Brufau, P. Miribel, A. Saiz-Vela, M. Puig, and J. Samitier, "Novel autonomous low power VLSI system powered by ambient mechanical vibrations and solar cells for portable applications in a 0.13μ technology," in *Proc. IEEE Power Electron. Specialists Conf.*, Orlando, FL, USA, Jun. 2007, pp. 2786–2791.
[10] J. Bito, R. Bahr, J. G. Hester, S. A. Nauroze, A. Georgiadis, and M. M. Tentzeris, "A novel solar and electromagnetic energy harvesting system with a 3-D printed package for energy efficient Internet-of-Things wireless sensors," *IEEE Trans. Microw. Theory Techn.*, vol. 65, no. 5, pp. 1831–1842, May 2017.
[11] Y. Zhang, S. Shen, C. Y. Chiu, and R. Murch, "Hybrid RF-solar energy harvesting systems utilizing transparent multiport micromeshed antennas," *IEEE Trans. Microw. Theory Techn.*, vol. 67, no. 11, pp. 4534–4546, Nov. 2019.
[12] R. Murch, C. Y. Chiu, and S. Shen, "Harnessing ambient RF waves for novel applications," in *Proc. IEEE Asia-Pacific Microw. Conf. (APMC)*, 2020, pp. 42–44.
[13] W. C. Brown, "The history of power transmission by radio waves," *IEEE Trans. Microw. Theory Techn.*, vol. 32, no. 9, pp. 1230–1242, Sep. 1984.

[14] Z. Zhang, H. Pang, A. Georgiadis, and C. Cecati, "Wireless power transfer—An overview," *IEEE Trans. Ind. Electron.*, vol. 66, no. 2, pp. 1044–1058, Feb. 2019.
[15] J. Barreto, G. Perez, A.-S. Kaddour, and S. V. Georgakopoulos, "A study of wearable wireless power transfer systems on the human body," *IEEE Open J. Antennas Propag.*, vol. 2, pp. 86–94, 2020.
[16] A. Kiourti et al., "Next-generation healthcare: Enabling technologies for emerging bioelectromagnetics applications," *IEEE Open J. Antennas Propag.*, vol. 3, pp. 363–390, 2022.
[17] N. Shariati, W. S. Rowe, J. R. Scott, and K. Ghorbani, "Multi-service highly sensitive rectifier for enhanced RF energy scavenging," *Sci. Rep.*, vol. 5, no. 1, pp. 1–9, May 2015.
[18] S. D. Assimonis, S.-N. Daskalakis, and A. Bletsas, "Sensitive and efficient RF harvesting supply for batteryless backscatter sensor networks," *IEEE Trans. Microw. Theory Techn.*, vol. 64, no. 4, pp. 1327–1338, Apr. 2016.
[19] P. N. Alevizos, G. Vougioukas, and A. Bletsas, "Nonlinear energy harvesting models in wireless information and power transfer," in *Proc. IEEE 19th Int. Workshop Signal Process. Adv. Wireless Commun. (SPAWC)*, Jun. 2018, pp. 1–5.
[20] M. Wagih, A. S. Weddell, and S. Beeby, "Characterizing and modelling non-linear rectifiers for RF energy harvesting," in *Proc. 19th Int. Conf. Micro Nanotechnol. Power Gener. Energy Conversion App. (PowerMEMS)*, Dec. 2019, pp. 1–5.
[21] S. Shen, C. Y. Chiu, and R. Murch, "A dual-port triple-band L-probe microstrip patch rectenna for ambient RF energy harvesting," *IEEE Antennas Wireless Propag. Lett.*, vol. 16, pp. 3071–3074, 2017.
[22] S. Shen, Y. Zhang, C. Y. Chiu, and R. Murch, "An ambient RF energy harvesting system where the number of antenna ports is dependent on frequency," *IEEE Trans. Microw. Theory Techn.*, vol. 67, no. 9, pp. 3821–3832, Sep. 2019.
[23] S. Shen, Y. Zhang, C.-Y. Chiu, and R. Murch, "A triple-band high-gain multibeam ambient RF energy harvesting system utilizing hybrid combining," *IEEE Trans. Ind. Electron.*, vol. 67, no. 11, pp. 9215–9226, Nov. 2020.
[24] S. Shen, Y. Zhang, C.-Y. Chiu, and R. Murch, "Directional multiport ambient RF energy-harvesting system for the Internet of Things," *IEEE Internet Things J.*, vol. 8, no. 7, pp. 5850–5865, Apr. 2021.
[25] U. Olgun, C. C. Chen, and J. L. Volakis, "Investigation of rectenna array configurations for enhanced RF power harvesting," *IEEE Antennas Wirel. Propag. Lett.*, vol. 10, pp. 262–265, 2011.
[26] H. Huang, Y. Liu, and S. Gong, "A novel dual-broadband and dual-polarized antenna for 2G/3G/LTE base stations," *IEEE Trans. Antennas Propag.*, vol. 64, no. 9, pp. 4113–4118, Sep. 2016.
[27] Y. Cui, L. Wu, and R. Li, "Bandwidth enhancement of a broadband dual-polarized antenna for 2G/3G/4G and IMT base stations," *IEEE Trans. Antennas Propag.*, vol. 66, no. 12, pp. 7368–7373, Dec. 2018.
[28] Z. Li, J. Han, Y. Mu, X. Gao, and L. Li, "Dual-band dual-polarized base station antenna with a notch band for 2/3/4/5G communication systems," *IEEE Antennas Wireless Propag. Lett.*, vol. 19, pp. 2462–2466, 2020.
[29] *3rd Generation Partnership Project; Technical Specification Group Radio Access Network; NR, E-UTRA, UTRA and GSM/EDGE; Multi-Standard Radio (MSR) Base Station (BS) Conformance Testing*, 3GPP Standard TS 37.141; Clause 6.2.1, 2020.
[30] "The office of the communications authority of the Government of the Hong Kong special administrative region." Accessed: Dec. 3, 2022. [Online]. Available: https://www.ofca.gov.hk/en/home/index.html
[31] M. Piñuela, P. D. Mitcheson, and S. Lucyszyn, "Ambient RF energy harvesting in urban and semi-urban environments," *IEEE Trans. Microw. Theory Techn.*, vol. 61, no. 7, pp. 2715–2726, Jul. 2013.
[32] D. Surender, M. A. Halimi, T. Khan, F. A. Talukdar, and Y. M. Antar, "A triple band rectenna for RF energy harvesting in smart city applications," *Int. J. Electron.*, to be published.
[33] D. Surender, M. A. Halimi, T. Khan, F. A. Talukdar, S. K. Koul, and Y. M. Antar, "2.45 GHz Wi-Fi band operated circularly polarized rectenna for RF energy harvesting in smart city applications," *J. Electromagn. Waves Appl.*, vol. 36, no. 3, pp. 407–423, 2022.
[34] D. Surender, T. Khan, F. A. Talukdar, A. De, Y. M. Antar, and A. P. Freundorfer, "Key components of rectenna system: A comprehensive survey," *IETE J. Res.*, vol. 68, no. 5, pp. 1–28, May 2020.
[35] D. Surender, T. Khan, F. A. Talukdar, and Y. M. M. Antar, "Rectenna design and development strategies for wireless applications: A review," *IEEE Antennas Propag. Mag.*, vol. 64, no. 5, pp. 16–29, Oct. 2022.
[36] C. R. Rowell and R. D. Murch, "A capacitively loaded PIFA for compact mobile telephone handsets," *IEEE Trans. Antennas Propag.*, vol. 45, no. 5, pp. 837–842, May 1997.
[37] "Mini-circuits." Accessed: Dec. 3, 2022. [Online]. Available: https://www.minicircuits.com/
[38] *CST Studio Suite*, Dassault Systèmes, Vélizy-Villacoublay, France, 2022.
[39] B. Clerckx and E. Bayguzina, "Low-complexity adaptive multisine waveform design for wireless power transfer," *IEEE Antennas Wireless Propag. Lett.*, vol. 16, pp. 2207–2210, 2017.
[40] F. Giannini, C. Paoloni, and M. Ruggieri, "CAD-oriented lossy models for radial stubs," *IEEE Trans. Microw. Theory Techn.*, vol. 36, no. 2, pp. 305–313, Feb. 1988.
[41] "Texas Instruments." 2021. [Online]. Available: https://www.ti.com/
[42] "TI evaluation module." Accessed: Dec. 3, 2022. [Online]. Available: https://www.ti.com/tool/BQ25570EVM-206
[43] "TI LaunchPad^{TM}." Accessed: Dec. 3, 2022. [Online]. Available: https://www.ti.com/tool/LAUNCHXL-CC2640R2
[44] "Bosch sensortec GmbH." Accessed: Dec. 3, 2022. [Online]. Available: https://www.bosch-sensortec.com/
[45] "Adafruit industries." Accessed: Dec. 3, 2022. [Online]. Available: https://www.adafruit.com/product/2652
[46] "Raspberry Pi," Accessed: Dec. 3, 2022. [Online]. Available: https://www.raspberrypi.com/
[47] R. J. Vyas, B. B. Cook, Y. Kawahara, and M. M. Tentzeris, "E-WEHP: A batteryless embedded sensor-platform wirelessly powered from ambient digital-TV signals," *IEEE Trans. Microw. Theory Techn.*, vol. 61, no. 6, pp. 2491–2505, Jun. 2013.
[48] S. Kim, R. Vyas, J. Bito, K. Niotaki, A. Collado, A. Georgiadis, and M. M. Tentzeris, "Ambient RF energy-harvesting technologies for self-sustainable standalone wireless sensor platforms," *Proc. IEEE*, vol. 102, no. 11, pp. 1649–1666, Nov. 2014.
[49] L. Yang, Y. J. Zhou, C. Zhang, X. M. Yang, X. X. Yang, and C. Tan, "Compact multiband wireless energy harvesting based battery-free body area networks sensor for mobile healthcare," *IEEE J. Electromagn. RF Microw. Med. Biol.*, vol. 2, no. 2, pp. 109–115, Jun. 2018.
[50] Z. Zeng et al., "Design of sub-Gigahertz reconfigurable RF energy harvester from -22 to 4 dBm with 99.8% peak MPPT power efficiency," *IEEE J. Solid-State Circuits*, vol. 54, no. 9, pp. 2601–2613, Sep. 2019.

MING-TAI CHIU received the B.Eng. degree in electronic engineering and the M.Phil. degree in electronic and computer engineering degree from The Hong Kong University of Science and Technology, Hong Kong, in 2020 and 2022, respectively.

He is currently working in the industry on signaling and telecommunications. His research interests include signaling, IoT, and energy harvesting.

CHI-YUK CHIU (Senior Member, IEEE) received the B.Eng., M.Eng., and Ph.D. degrees in electronic engineering from the City University of Hong Kong, in 2001, 2001, and 2005, respectively.

He joined the Department of Electronic and Computer Engineering (ECE), The Hong Kong University of Science and Technology (HKUST) as a Research Associate in 2005. Then, he worked with Sony Mobile Communications, Beijing, as a Senior Antenna Engineer in 2011. He again joined as a Research Assistant Professor with the ECE, HKUST, in 2015. He has published over 100 technical papers, two book chapters and holds several patents related to antenna technology. His main research interests include the design and analysis of small antennas, MIMO antennas, applications of characteristic modes, and energy harvesting. He is the Vice Chair of IEEE Antennas and Propagation Society/Microwave Theory and Technology Society Hong Kong Joint Chapter, a member of IEEE AP-S Education Committee, IEEE AP-S C. J. Reddy Travel Grant Assistant Coordinator, and a Lead Guest Editor of a special section in IEEE OPEN JOURNAL OF ANTENNAS AND PROPAGATION.

CHARLES NG received the Bachelor of Engineering degree in electronic engineering and minor in sustainable energy engineering from The Hong Kong University of Science and Technology (HKUST) in 2019, where he is currently pursuing the master's degree in electronic and computer engineering.

He was a Research Assistant with HKUST from 2020 to 2022, participating in research projects on reconfigurable antenna for wireless communications. His current research interests include antenna design and energy harvesting for radio frequency.

LAP-ON WONG received the bachelor's degree in electronic engineering with a minor in information technology from The Hong Kong University of Science and Technology in 2021, where he is currently pursuing the M.Phil. degree in electronic and computer engineering. His research interests include RF imaging and ambient RF energy harvesting.

SHANPU SHEN (Member, IEEE) received the bachelor's degree in communication engineering from the Nanjing University of Science and Technology, Nanjing, China, in 2013, and the Ph.D. degree in electronic and computer engineering from The Hong Kong University of Science and Technology (HKUST), Hong Kong, in 2017.

He was a Visiting Ph.D. student with the Microsystems Technology Laboratories, Massachusetts Institute of Technology, Cambridge, MA, USA, in 2016. He was a Postdoctoral Fellow with HKUST from 2017 to 2018, and a Postdoctoral Research Associate with the Communications and Signal Processing Group, Imperial College London, London, U.K., from 2018 to 2020. He is currently a Research Assistant Professor with HKUST. His current research interests include RF energy harvesting, wireless power transfer, reconfigurable intelligent surface, Internet-of-Things, MIMO systems, and antenna design and optimization.

ROSS MURCH (Fellow, IEEE) received the bachelor's and Ph.D. degrees in electrical and electronic engineering from the University of Canterbury, New Zealand.

He is currently a Chair Professor with the Department of Electronic and Computer Engineering and a Senior Fellow with the Institute of Advanced Study, The Hong Kong University of Science and Technology, where he was the Department Head from 2009 to 2015. He has been a David Bensted Fellow, Simon Fraser University, Canada, and a HKTIIT Fellow with Southampton University, U.K., and has spent sabbaticals at MIT, USA; AT&T, USA; Allgon Mobile Communications, Sweden; and Imperial College London. He has successfully supervised over 50 research graduate students and his research contributions include more than 175 journal papers and 20 patents. His unique expertise lies in his combination of knowledge from both wireless communication systems and electromagnetics and he publishes in both areas. His current research interests include RF imaging, ambient RF systems, energy harvesting, multiport antenna systems Internet of Things, and reconfigurable intelligent surfaces.

Prof. Murch has won several awards, including the Computer Simulation Technology University Publication Award. He enjoys teaching and has won three teaching awards. He has served IEEE in various positions, including IEEE area editor, technical program chair, distinguished lecturer, and Fellow evaluation committee. He is a Fellow of IET and HKIE.